Turkish Journal of Nuclear Science (2022), Vol. 34, No.1. Page: 1-15 http://dergipark.gov.tr/tjins

MEASUREMENT OF S-FACTOR FOR THE $^{11}B(p, \alpha)2\alpha$ REACTION AT LOW ENERGIES: CARBON BUILD-UP EFFECT

Osman ALAÇAYIR[1)], Nilgün BAYDOĞAN[2)], Tamer YALÇIN[1)], Adnan BAYKAL[1)], Recep BIYIK[1*)]

1) Turkish Energy, Nuclear and Mineral Research Agency, Nuclear Energy Research Institute, Küçükçekmece, 34303 İstanbul/TÜRKİYE

2) Istanbul Technical University, Energy Institute, Maslak, 34469 İstanbul/TÜRKİYE

*recep.biyik@tenmak.gov.tr

DÜŞÜK ENERJİLERDE $^{11}B(p, \alpha)2\alpha$ REAKSİYONU İÇİN S-FAKTÖRÜNÜN ÖLÇÜMÜ: KARBON BUILD-UP ETKİSİ

Abstract:

The astrophysical S-factor for the $^{11}B(p, \alpha)2\alpha$ reaction has been evaluated at effective center of mass (CM) energies of 110, 113, 115, 117, 119, 121, 124, 126, 128, 131, and 133 keV. It was observed that there was a significant difference between the calculated values and the literature values. Another difference with literature is the increased yield ratio N_0/N_1 of the reaction channels $^{11}B(p,\alpha_0)^8Be$ and $^{11}B(p,\alpha_1)^8Be$ with increasing energy. The reason for the discrepancy was attributed to being carbon build-up on the target surface during irradiation. Due to the Carbon build-up effect in the energy range studied, effective energy (E_{eff}) values for the $^{11}B(p, \alpha)2\alpha$ reaction decreased by about 30 keV.

Özet:

$^{11}B(p, \alpha)2\alpha$ reaksiyonu için astrofiziksel S faktörü, 110, 113, 115, 117, 119, 121, 124, 126, 128, 131 ve 133 keV etkin kütle merkezi (CM) enerjilerinde değerlendirilmiştir. Hesaplanan değerler ile literatür değerleri arasında anlamlı bir farklılık olduğu görülmüştür. Literatürle olan diğer bir fark, artan enerji ile $^{11}B(p,\alpha_0)^8Be$ ve $^{11}B(p,\alpha_1)^8Be$ reaksiyon kanallarının N_0/N_1 verim oranının artmasıdır. Elde edilen değerlerin literatür değerleri ile farklılaşmasının nedeni, ışınlama sırasında hedef yüzeyde uluşan karbon birikmesine atfedildi. İncelenen enerji aralığındaki karbon birikimi etkisi nedeniyle, $^{11}B(p, \alpha)2\alpha$ reaksiyonu için etkin enerji (E_{eff}) değerleri yaklaşık olarak 30 keV azaldığı görüldü.

Keywords: S-factor, carbon build-up, $^{11}B(p, \alpha)^8Be$, $^{11}B(p, \alpha)2\alpha$ reaction,

Anahtar Kelimeler: S-faktörü, Karbon build-up, $^{11}B(p, \alpha)^8Be$, $^{11}B(p, \alpha)2\alpha$ reaksiyonu,

1. Introduction

The $^{11}B(p,\alpha)^8Be$ reaction has been the focus of researchers since the 1930s and was first studied by Oliphant and Rutherford (Oliphant & Rutherford, 1933). Interest in the reaction tends to increase in recent years, with the increasing number of studies on aneutronic fusion (Belyaev et al., 2015, Wessel et al., 2000). Contrary to conventional fusion reactors where D-T reaction is used, $^{11}B(p,\alpha)^8Be$ appears to be more advantageous in terms of radioactive

Corresponding author: Recep BIYIK, Turkish Energy, Nuclear and Mineral Research Agency, Nuclear Energy Research Institute, Küçükçekmece, 34303 İstanbul/TÜRKİYE, E-mail:recep.biyik@tenmak.gov.tr ORCID:0000-0001-7929-4395
Gönderim: 21/02/2022 Kabul: 28/06/2022.

contamination since there are no neutrons generated in the reactors utilizing this reaction. Another reason for the interest in the reaction is the need to know the reaction rates of this reaction in order to understand the relative abundances of B, Li, and Be in astrophysical studies (Boesgaard et al., 2005, Lamia et al., 2011).

Techniques such as nuclear reaction analysis (NRA), Rutherford backscattering spectrometry (RBS), heavy ion recoil detection analysis (HERDA) are used to determine the distribution of elements on various material surfaces. NRA is used in conjunction with the RBS as a complementary method. Its sensitivity in light elements is the advantage of NRA over RBS. Depth analysis of light elements can be performed at the nanometer (nm) level thanks to NRA. NRA using the $^{11}B(p,\alpha_0)^8Be$ reaction has two important advantages; having a high cross-section and an alpha peak that is completely isolated from the energy of protons impinged on the surface, thus minimizing the margin of error arising from data analysis (Kokkoris et al., 2010), (Mayer et al., 1998). Furthermore, the experimental method used in NRA and RBS is almost the same with the method used in the present study. This increases the importance of the present study to gain infrastructure for some ion beam applications (IBA) like NRA and RBS.

The $^{11}B(p,3\alpha)$ reaction basically has the possibility to occur through three different channels;

Channel.1 $p+^{11}B \rightarrow ^{12}C^* \rightarrow ^{8}Be+\alpha_0 \rightarrow \alpha_{01}+\alpha_{02}+\alpha_0$

Channel.2 $p+^{11}B \rightarrow ^{12}C^* \rightarrow ^{8}Be^*+\alpha_1 \rightarrow \alpha_{11}+\alpha_{12}+\alpha_1$

Channel.3 $p+^{11}B \rightarrow ^{12}C^* \rightarrow \alpha_{21}+\alpha_{22}+\alpha_{23}$

Channels 1 and 2 are called sequential reactions, while channel 3 is called direct reactions. No evidence was found in the analyses that the reaction took place through the 3rd channel. All findings point to sequential decay. While the decays occur in the 1st channel to the ground state energy level of the ^8Be nucleus, the reactions from the 2nd channel take place to the 1st excited level of the ^8Be nucleus (Becker et al., 1987).

In this study, S-Factor of the $^{11}B(p,\alpha_0)^8Be$ and $^{11}B(p,\alpha_1)^8Be^*$ reaction channels at effective energy range 110-133 keV (CM) and at 135º detector angle was measured. The energies are effective CM energies calculated by considering the stopping power of the thick target ($56\mu g/cm^2$) used in the experiment. Yield ratios of the first and second reaction channels are calculated for the energies studied. When the S-factor values, obtained in this study, were compared with the literature values, there is a significant difference. It was considered that the carbon build-up effect was the reason for the difference and according to the results, this effect causes approximately 30 keV to decrease E_{eff} values at the energy range studied.

Carbon build-up is the accumulation of some organic compounds on surfaces irradiated with ions in ion beam applications. This effect mainly occurs because of some hydrocarbons and other gases like CO, CO_2, H_2O etc. remained in the vacuum chamber. These gases are usually vapors of vacuum pump oils or vacuum greases and gases released from o-rings, the walls of the vacuum chamber etc.. The other most important reason for carbon build-up is the various organic residues accumulated on the target material that is not cleaned sufficienly before irradiation.

2. Experimental

Irradiations were carried out in the SAMES J-15 ion accelerator installed in Nuclear Energy Research Institute (NUKEN), Istanbul. SAMES J-15 accelerator is a Van de Graff type accelerator with a maximum voltage of 150 kV (Fig. 1). The ion source is an RF type with an extraction voltage of 5kV. A detailed explanation about J-15 Accelerator can be found at the (Alaçayır, 2015, Baykal, 1997, Tarcan et al., 1998).

The scattering chamber (Alaçayır, 2015, Baykal, 1997) experimental set-up, and counting system are shown in Figure 2. The scattering chamber is a cylindrical vacuum chamber made of stainless steel with a diameter of approximately 250 mm and a depth of 85 mm. The target holder placed in the centre can be moved vertically thanks to a rotary-linear feedthrough without disturbing the vacuum, so that different points of the target can be irradiated. The target holder can be rotated around its own axis so that the beam angle can be adjusted. Two surface-barrier detectors can be placed inside the vacuum chamber, one of which is fixed and the other can be rotated 360° around the target with the help of a rotary feedthrough.

Figure 1. Low Energy Ion Accelerator- Sames J-15 and Van-de Graaff Generator

The collimators consist of three consecutive metal bracelets with an inner diameter of 3 mm. The current read in the micrometer, which gives the collimator current since they are in contact with each other, is the total current value of the three collimators. There is an electron

suppresser ring in front of the target with an inner diameter of 10 mm (Fig. 2, *a*). The suppresser ring has a voltage of -180V while irradiations. A Beaudouin oil backing pump and an Edwards B04 model oil diffusion pump were used to maintain the vacuum in the beamline and scattering chamber at 5.0x 10^{-6} Torr during irradiation. Detection of alpha particles formed in the reaction was carried out with a 300 mm^2 surface barrier detector (Ametec-Ortec U-016-300-100, Ultra Ion-Implanted Detector) (Fig. 2, *b*). In the counting system, an Ortec 401B Bin, an Ortec 428 detector bias supply, a Canberra 2003B model preamplifier, a Canberra 2020 model amplifier, and a Canberra Multiport-II multichannel analyzer (MCA) were used (Fig. 2, *b*).

Irradiations were carried out at 5µA beam current for 4250 s. Beam current is measured during the irradiation with an Ortec 439 digital current integrator and an Ortec 875 Counter. On the other hand, because the beam energy was not sufficient, energy calibration could not be done for the accelerator. Hence the projectile/proton energy is taken directly as the high voltage value plus extraction voltage. The high voltage was measured with an error less than 1.0 keV.

After each irradiation, the target was shifted, and it has been ensured that all irradiations are carried out with a fresh target. The targets to be irradiated were prepared by thermal evaporation of natural B_2O_3 on thin aluminium foil at a pressure environment of 10^{-4} Torr. The target thickness was calculated as 56 µg/cm^2 as a result of the measurements made before and after coating.

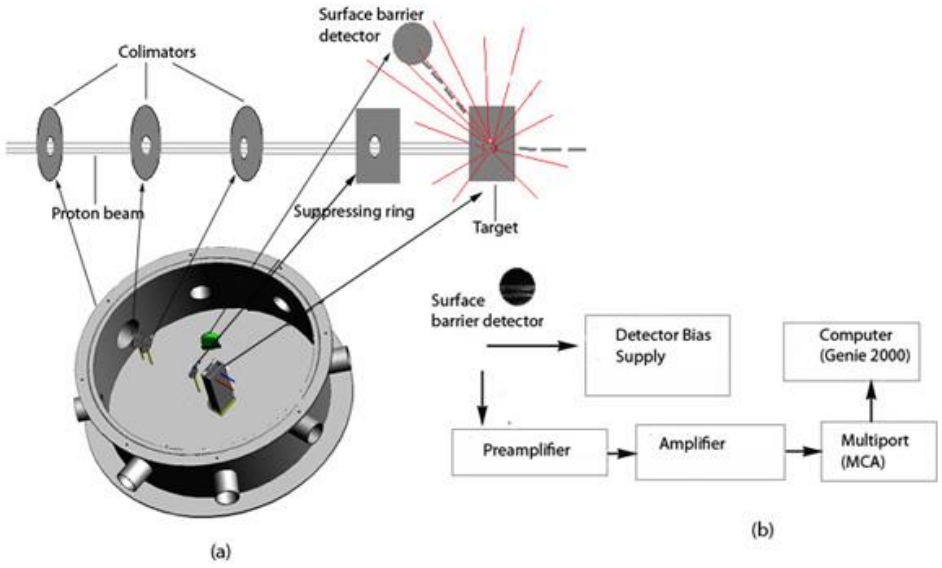

Figure 2. a) Experimental set up, scattered chamber (collimators, electron suppresser, target, and surface barrier detector) b) and counting system

Calibration of the surface-barrier detector was performed with an Amersham calibration source, consisting of Americium-241, Curium-244, Plutonium-239 isotopes (Amersham, 1992). Since the alpha counts caused by the vacuum environment are close to zero and the alpha counts caused by the reaction are only a few per second, the detector efficiency is accepted as 100%. The detector is placed at an angle of 135° with the direction of the beam. In order to prevent the photons scattered from the target from reaching the detector, a thin 250 µg/cm^2 aluminized mylar foil was used.

The solid angle is calculated assuming the target is closer to the elliptic geometry. Sacalc-Ellipsoid computer software (Whitcher, 2014) using the Monte Carlo method was used. Cross-section data calculated using the solid angle value resulting from the elliptic target approach were compared with the values in the literature.

3. Results and discussion

The alpha (α) particles emitted from the $^{11}B(p,\alpha)2\alpha$ reaction as a result of irradiation of the B_2O_3 target with protons at energies of 110-133 keV were counted with a surface-barrier detector. The alpha spectrum with different energies has been visualized with the Genie 2000 program. Alpha particle spectra have been obtained at effective CM energies 110, 113, 115, 117, 119, 121, 124, 126, 128, 131, 133 keV. As an example, the alpha spectrum for proton beam energy at 115 keV was given in Fig. 3. Although the counts at 115 keV proton energies is greater than the counts at the other energies it doesn't mean anything if the size of the error bars are considered (Fig.5). In the literature, although the cross section values are increased regularly in direct proportion to projectile/proton energy, it seems our values are irregular.

The reason for this situation can be shown as the low homogeneity of the target thickness and the different Carbon build-up thickness for each irradiation. Since the α_0 peak is completely separate from the spectrum, the number of α_0 particles (N_0) was calculated directly using this peak. On the other hand, the α_1 peak is unfortunately intertwined with the secondary alpha counts. Since three particles are created after the reaction, one of which is the primary alpha particle (α_1) and the other two is secondary alpha particles (α_{11} and α_{12}), the total number of α_1 particles (N_1) was calculated by taking 1/3 of the total count in the spectrum (Stave et al., 2011, Davidson et al., 1979). As seen in the spectra, the low-energy region of the spectrum was cut to avoid electronic noise. The counts in this region were calculated by the extrapolation method (Fig. 4).

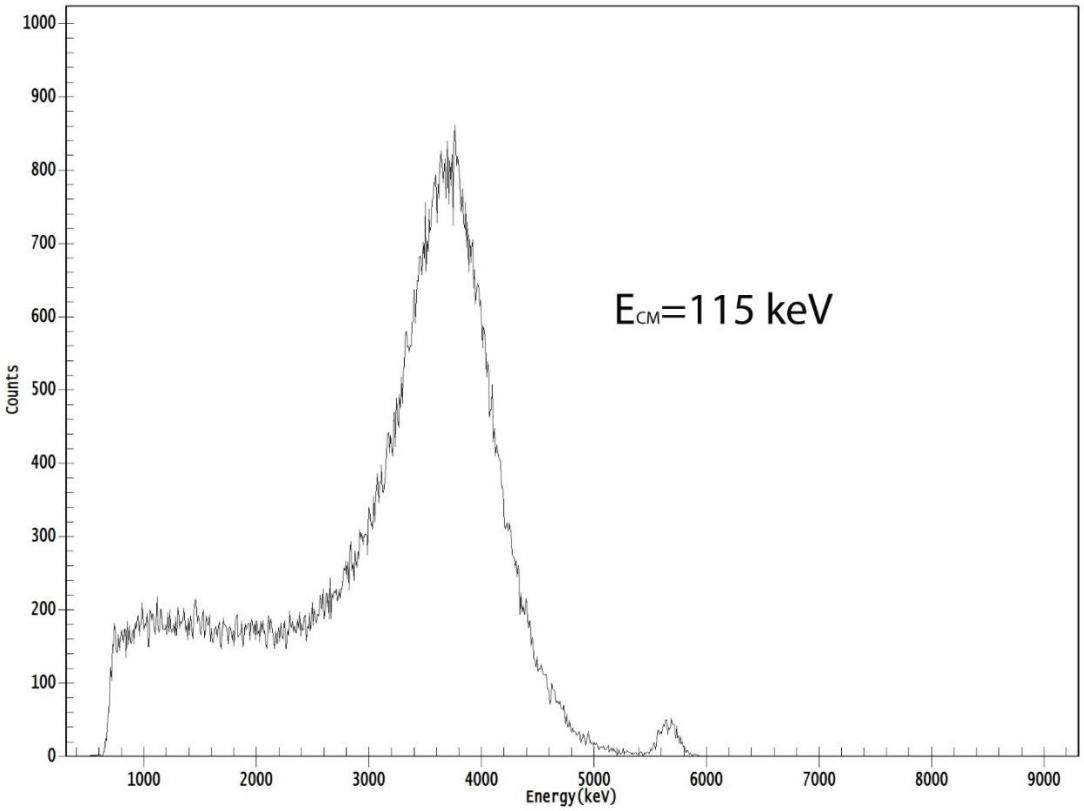

Figure 3. The alpha spectrum at E_{CM} 115 keV of $^{11}B(p,\alpha)2\alpha$ reaction, the low energy region of the spectrum was cut to avoid the electronic noise.

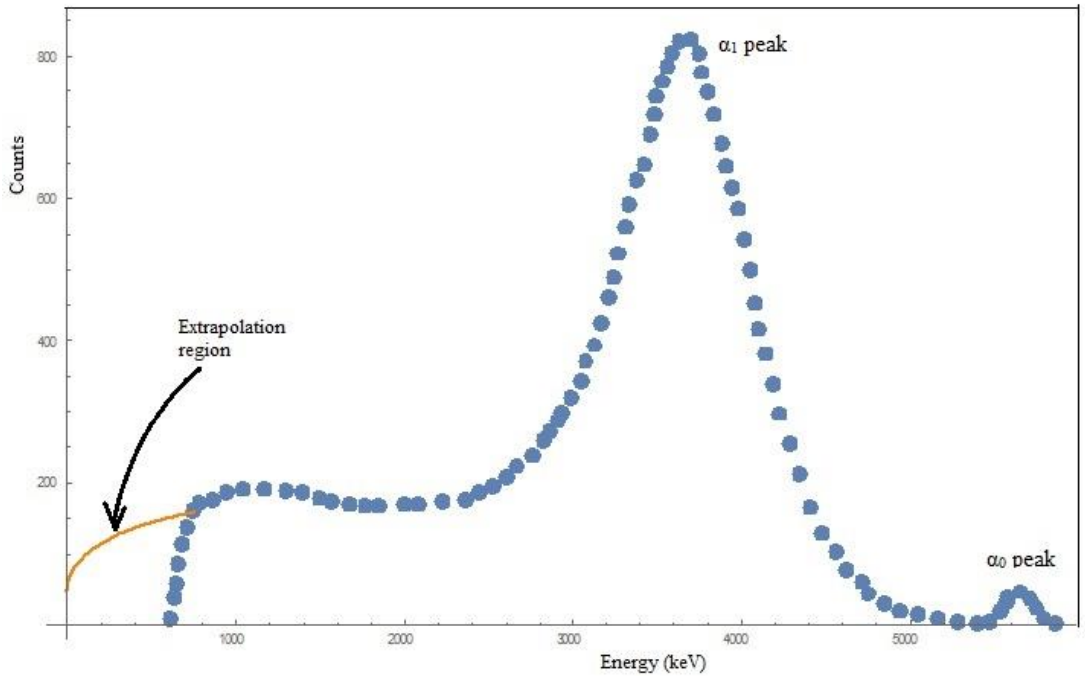

Figure 4. Alpha energy spectrum and extrapolation region

To determine the uncertainty in target thickness, different points of the target were bombarded with 117 keV (CM) energy protons. The α_0 yield was determined directly by taking the total counts under the α_0 peak in the obtained alpha spectra. The total uncertainty was

calculated by taking the square root of the sum of the squares of the uncertainty that comes from the direct measuring of the target thickness and the uncertainty obtained from these counts.

The Stopping Range of Ions in Matter (SRIM) tables (Ziegler et al., 2010) were used to calculate the energy loss of protons in the target. Then the effective energy of the protons in the target was found by iterative calculations using the expression (Angulo et al., 1993)

$$\int_{E_0-\Delta}^{E_0} \sigma(E)\varepsilon(E)^{-1}dE = 2\int_{E_{eff}}^{E_0} \sigma(E)\varepsilon(E)^{-1}dE \quad (1)$$

where σ(E) is the cross-section of the reaction at the CM Energy E. Here a function σ(E) has been formed at these energies by fitting the data of Ref. (Becker et al., 1987). ε(E) is the stopping power of protons in the target at the CM Energy E. A function has been fitted here too, using the SRIM data. E_0 is the initial CM energy before entering the target. Δ is the energy loss of the beam, E_{eff} is the effective beam energy at the target.

Uncertainty in the effective energy $\Delta(E_{eff})$ is found as 9 keV which is calculated by the expression

$$\Delta(E_{eff}) = \sqrt{\frac{1}{N}\int_{E_0-\Delta}^{E_0}(E - E_{eff})^2\sigma(E)dE} \quad (2)$$

where N is normalization constant which can be shown as;

$$N = \int_{E_0-\Delta}^{E_0} \sigma(E)dE \quad (3)$$

Here again, the function used at Eq. (1) has been used as σ(E).

The partial cross-sections at these energies have been calculated using the expression;

$$\sigma(E_{eff}) = 4\pi\,(n_\alpha\, cos\Theta) \,/\, (I\, n_0\, \Omega) \quad (4)$$

where

$\sigma(E_{eff})$: Partial cross-section at effective CM energy E_{eff}

E_{eff} : Effective CM energy

n_α : Number of alpha particles counted

I : Number of protons arrived at the target

n_0 : Number of ^{11}B nucleus per unit surface (cm^2)

Ω : Solid angle (steradians)

Θ : The angle between the target normal and the beam direction ($\theta = 0^0$)

Two different S-Factor sets have been calculated. The first one is for $^{11}B(p,\alpha_0)^8Be$ channel (Fig.5) which was compared with (Becker et al., 1987), (Spitaleri et al., 2004) and the second one is for $^{11}B(p,\alpha_1)^*{}^8Be$ channel (Fig. 6) which was compared with (Becker et al., 1987), (Angulo et al., 1993).

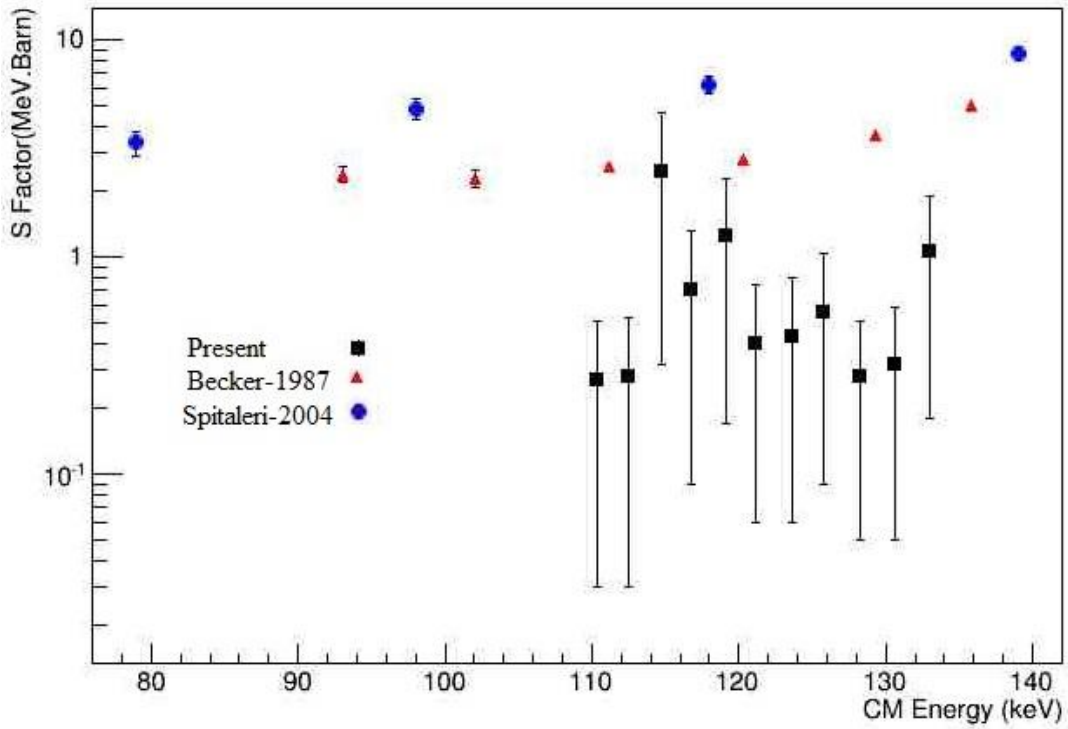

Figure 5. Calculated S-factor of the $^{11}B(p,\alpha_0)^8Be$ channel and compared with (Becker et al., 1987), (Spitaleri et al., 2004)

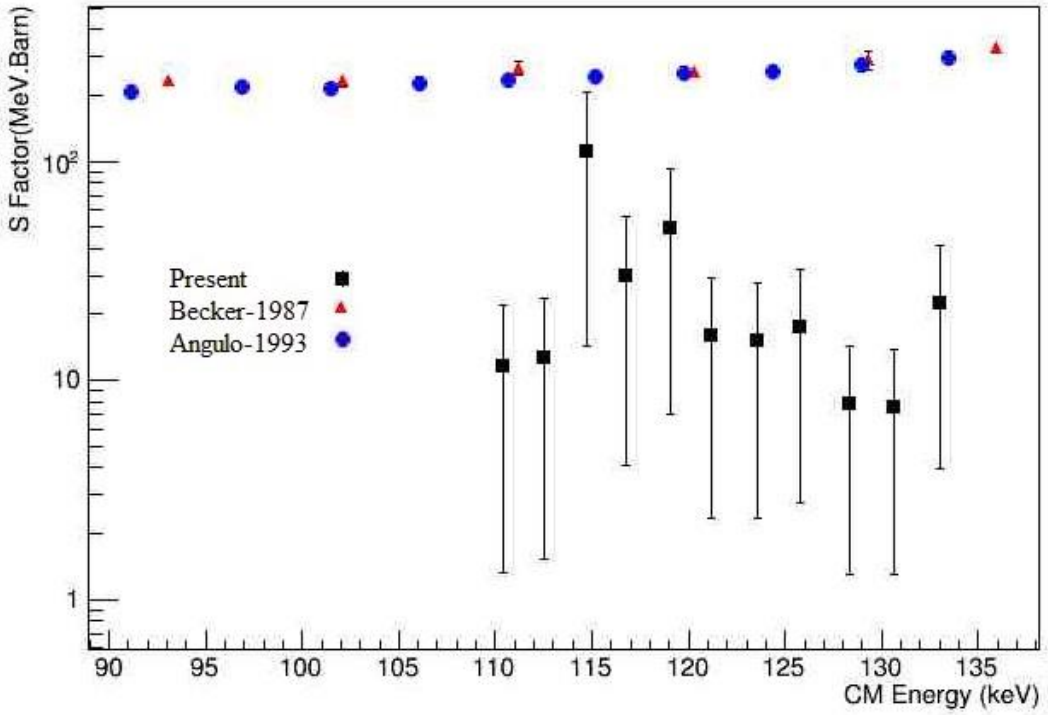

Figure 6. Calculated S-factor of the $^{11}B(p,\alpha_1)^*{}^8Be$ channel and compared with (Becker et al., 1987), (Angulo et al., 1993)

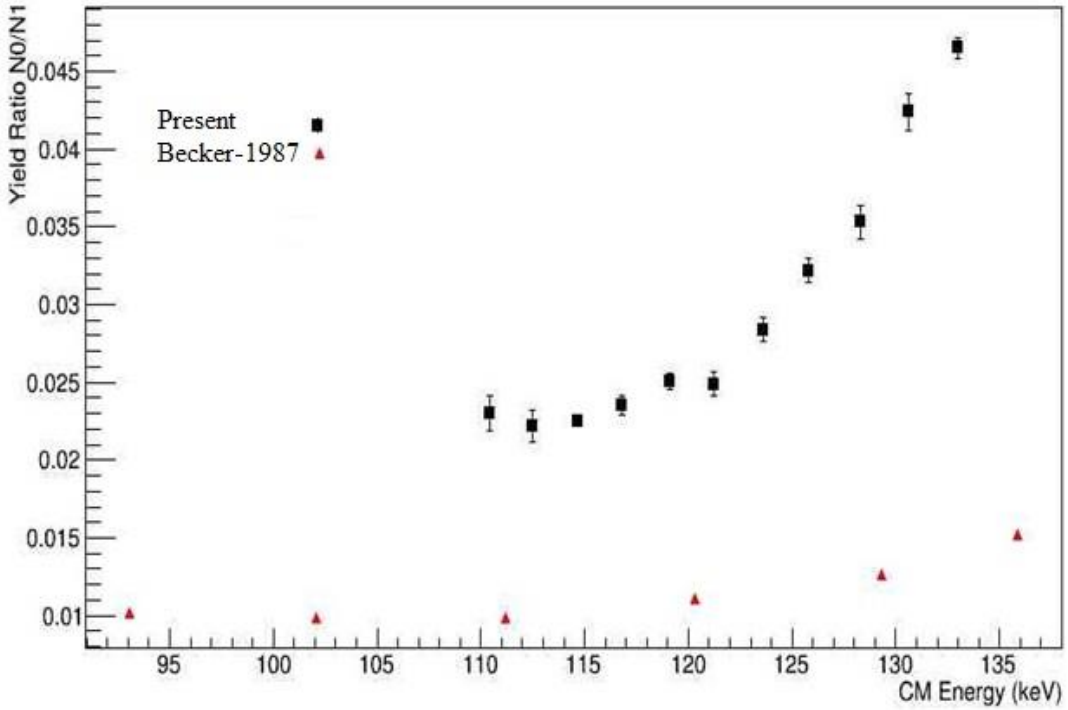

Figure 7. Yield ratio N_0/N_1 of the reaction channels $^{11}B(p,\alpha_0)^8Be$ and $^{11}B(p,\alpha_1)^8Be$.

The S-Factor has been calculated by the expression

$$S(E_{eff}) = \sigma(E_{eff})\ E_{eff}\ exp(2\pi\eta) \quad (5)$$

where

$S(E_{eff})$:S-factor at effective CM energy Eff

η :Sommerfeld parameter

When the S-factor values obtained in this study are compared with the literature values, it is observed that there is a significant difference. It has been evaluated that this may be due to Carbon build-up on the target surface during irradiation. Two factors were effective in reaching this conclusion. First; When the irradiated targets are examined, a brown-black darkening is observed in the irradiated region (Fig.8). Latter; Although the reason could not be understood during the irradiation, it was observed that the number of alpha particles reaching the detector decreased over time and almost no particles came towards the end of the irradiation.

Figure 8. Brown-black darkening in the irradiated region

The particles in the beam lost their energy by passing through this Carbon layer before reaching the ^{11}B nuclei. The calculated effective CM energy may be much less than the actual generated effective CM energy. This may have caused the calculated S-factor values to be less than expected.

When the E_{eff}(CM) values in this study are decreased by about 30 keV (Fig. 9), it is seen that the S-factor values corresponding to these energies are compatible with the values in (Becker et al., 1987). Based on this, it can be said that the proton beam lost about 30 keV of energy before reaching the ^{11}B target. By assuming a Carbon, Hydrogen and Oxygen accumulation on the target with a stoichimetric ratio 3:2:1 respecticely (Healy, 1997) with a stopping power of 0.59 keV/μg/cm^2 this means an average accumulation of 51.28 μg/cm^2. It must be noted that while calculating the 51.28 μg/cm^2 value obtained here, the gradual accumulation of Carbon was neglected, and it was assumed that the proton beam encountered the same Carbon layer thickness throughout the entire irradiation. Therefore, the amount of Carbon deposited at the end of the irradiation is actually more than the average value of 51.28 μg/cm^2.

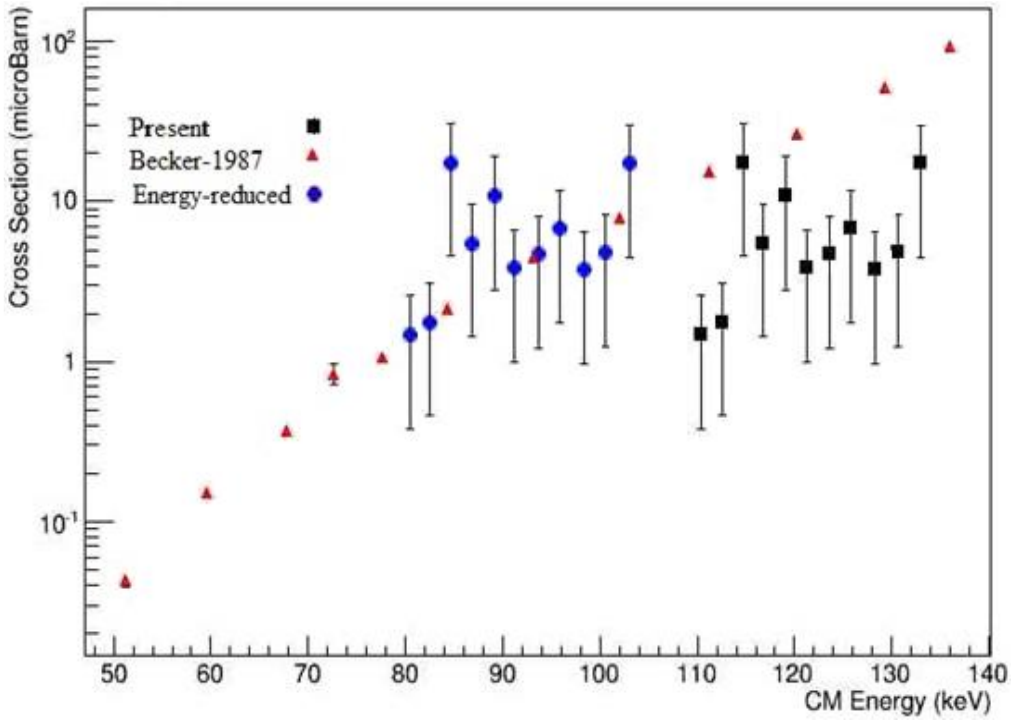

Figure 9. The cross-section data of $^{11}B(p,\alpha_0)^{8}Be$ reaction. Energy reduced values were compatible with (Becker et al., 1987)

Some calculations were evaluated to see if a Carbon build-up of 51.28 μg/cm^2 was possible. Moller et al., was investigated Carbon deposition on Ni surfaces bombarded with H^+, He^+ and Li^+ ions (Möller et al., 1981). In this study, the authors carried out their experiments at a pressure of 10^{-6} mbar and measured the amount of Carbon deposited on the surfaces using the $^{12}C(d,p)^{13}C$ reaction. In Fig.4 of (Möller et al., 1981), the amount of Carbon accumulation obtained depending on the irradiation dose is given according to different ion types. In the figure:

j : ion current and

j/W : the number of ions arrived to the surface per carbon atoms formed.

When the (c) part of the figure is examined, it can be said that roughly one Carbon atom is accumulated for each ion on the surfaces bombarded with H^+ ions with 100 keV energy, at irradiation doses up to $0.5x10^{14}$ ions/s corresponding to 8 μA.

For recent study by using the formulas:

$$N' = {}^{N}/_{S} = N_1 \, {}^{t}/_{S} = {}^{({}^{I}/_{e})t}/_{(\pi ab)} \tag{6}$$

and,

$$d = \frac{1}{3}\left(\frac{N'}{N_A}\right) M \tag{7}$$

Where;

N: the total number of ions hitting the target during the irradiation

S: the irradiated surface area which is an ellips with dimentions a = 0.25 cm, b = 0.07cm

N_1: The ions arrived the target per unit time

t: the irradiation time (4250 s.)

I: the ion current (5 μA)

e: elementary charge ($1.6*10^{-19}$)

d: thickness of the Carbon accumulation ($\mu g/cm^2$)

N_A: Avogadro's number

M: Molar mass of the C_3H_2O (54 g/mole)

It can be found that the number of ions per unit surface and consequently the number of Carbon atoms accumulated on the target is $N'=2.42*10^{18}$ atoms/cm^2 which corresponds to a thikness of d=72.36 $\mu g/cm^2$. This value is greater than 51.28 $\mu g/cm^2$ value. But as it be noted before, 51.28 $\mu g/cm^2$ is not the final thickness but the average thickness, the protons encountered. Of course the final thickness is actually greater than the average one.

Yield ratio N_0/N_1 of the reaction channels $^{11}B(p,\alpha_0)^8Be$ and $^{11}B(p,\alpha_1)^8Be$ is given in (Fig. 7). It seems N_0/N_1 values obtained in present work are greater than those of (Becker et al., 1987). To calculate N_1 we have taken one third of total number of α_1, α_{11} and α_{12}. But α_{11} and α_{12} particles have less energy compared to α_0 particles. Hence these particles can easily be absorbed by the Carbon layer and the number of α_{11} and α_{12} particles arrived to the detector be decreased, which can effect N_1 negatively, while the number of α_0 particles (N_0) have been unaffected. That is why N_0/N_1 obtained in this study is greater than that of (Becker et al., 1987).

4. Conclusions

It was observed that there was a significant difference between the S-factor values measured in this work and the literature values. The reason for these differences was considered to be Carbon build-up on the target surface during irradiation. On average, it has been calculated that the proton beam encounters a Carbon build-up of 51.28 $\mu g/cm^2$ before reaching the target.

When the alpha spectra are examined, it can be said that the cross-section of the $^{11}B(p,\alpha_0)^8Be$ reaction channel increases with beam energy faster than that of $^{11}B(p,\alpha_1)^8Be$. In this study, it has been found that the yield ratio N_0/N_1 of the reaction channels $^{11}B(p,\alpha_0)^8Be$ and $^{11}B(p,\alpha_1)^8Be$ is greater than that of literature. This result is attributed to that the alpha particle (α_{11}, α_{12}) energies of the $^{11}B(p,\alpha_1)^8Be$ reaction channel is small, so that some of them can't penetrate out of the Carbon layer and can't arrive the detector which decreases N_1 and consequently increases N_0/N_1.

Acknowledgments

This study was supported by the Turkish Energy, Nuclear, and Mineral Agency with Project Code A2.H4.F3.

References

1) Alaçayır, O. (2015). Measurement of Partıal Differential Cross Sections of the 11B(p,α)2α Reaction Occured by Bombardıng B2O3 Target wıth 103-127 keV Protons. MSc. Thesis, Istanbul Technical University.

2) Amersham. (1992). Certificate of calibration of alpha emitting radioactive reference source. A 3583(Calibration No: 0146).

3) Angulo, C., Engstler, S., Raimann, G., Rolfs, C., Schulte, W. H. & Somorjai, E. (1993). The effects of electron screening and resonances in (p, α) reactions on10B and11B at thermal energies. Zeitschrift Für Physik A Hadrons and Nuclei, 345(2), 231–242. https://doi.org/10.1007/BF01293350.

4) Baykal, A. (1997). Li+d reaction at low energies. Doctorate Thesis, Istanbul University.

5) Becker, H. W., Rolfs, C. & Trautvetter, H. P. (1987). Low-energy cross sections for11B(p, 3α). Zeitschrift Für Physik A Atomic Nuclei, 327(3), 341–355. https://doi.org/10.1007/BF01284459.

6) Belyaev, V. S., Krainov, V. P., Matafonov, A. P. & Zagreev, B. V. (2015). The new possibility of the fusion p $\mathplus$11B chain reaction being induced by intense laser pulses. Laser Physics Letters, 12(9), 96001. https://doi.org/10.1088/1612-2011/12/9/096001.

7) Boesgaard, A. M., Deliyannis, C. P. & Steinhauer, A. (2005). Boron Depletion in F and G Dwarf Stars and the Beryllium-Boron Correlation. The Astrophysical Journal, 621(2), 991–998. https://doi.org/10.1086/427687.

8) Davidson, J. M., Berg, H. L., Lowry, M. M., Dwarakanath, M. R., Sierk, A. J. & Batay-Csorba, P. (1979). Low energy cross sections for 11B(p, 3α). Nuclear Physics, Section A, 315(1–2), 253–268. https://doi.org/10.1016/0375-9474(79)90647-X.

9) Healy, M. J. F. (1997). Minimising carbon contamination during ion beam analysis. Nuclear Instruments and Methods in Physics Research Section B: Beam Interactions with Materials and Atoms, 129(1), 130–136. https://doi.org/https://doi.org/10.1016/S0168-583X(97)00127-4.

10) Kokkoris, M., Kafkarkou, A., Paneta, V., Vlastou, R., Misaelides, P. & Lagoyannis, A. (2010). Differential cross sections for the 11B(p,αo) 8Be and 11B(p,p0)11B reactions, suitable for ion beam analysis. Nuclear Instruments and Methods in Physics Research, Section B: Beam Interactions with Materials and Atoms, 268(24), 3539–3545. https://doi.org/10.1016/j.nimb.2010.09.013.

11) Lamia, L., Spitaleri, C., Burjan, V., Carlin, N., Cherubini, S., Crucillà, V., Munhoz, M. G., Santo, M. G. Del, Gulino, M., Hons, Z., Kiss, G. G., Kroha, V., Kubono, S., Cognata, M. La, Li, C., Mrazek, J., Mukhamedzhanov, A., Pizzone, R. G., Puglia, S. M. R. & Zhou, S. H. (2011). New measurement of the11B(p,$\upalpha$0)8Be bare-{nucleusS}(E) factor via the Trojan horse method. Journal of Physics G: Nuclear and Particle Physics, 39(1), 15106. https://doi.org/10.1088/0954-3899/39/1/015106.

12) Mayer, M., Annen, A., Jacob, W. & Grigull, S. (1998). The 11B(p,α0)8Be nuclear reaction and 11B(p,p)11B backscattering cross sections for analytical purposes. Nuclear Instruments and Methods in Physics Research, Section B: Beam Interactions with Materials and Atoms, 143(3), 244–252. https://doi.org/10.1016/S0168-583X(98)00383-8.

13) Möller, W., Pfeiffer, T. & Schluckebier, M. (1981). Carbon buildup by ion-induced polymerization under 100-400 keV H, He and Li bombardment. Nuclear Instruments and Methods, 182–183(PART 1), 297–302. https://doi.org/10.1016/0029-554X(81)90703-5.

14) Oliphant, M. L. E. & Rutherford, Lord. (1933). Experiments on the Transmutation of Elements by Protons. Proceedings of the Royal Society of London. Series A, Containing Papers of a Mathematical and Physical Character, 141 (843), 259–281. http://www.jstor.org/stable/96218.

15) Spitaleri, C., Lamia, L., Tumino, A., Pizzone, R. G., Cherubini, S., Del Zoppo, A., Figuera, P., La Cognata, M., Musumarra, A., Pellegriti, M. G., Rinollo, A., Rolfs, C., Romano, S. & Tudisco, S. (2004). The 11B(p, α0)8Be reaction at sub-Coulomb energies via the Trojan-horse method. Physical Review C-Nuclear Physics, 69 (5), 1–11. https://doi.org/10.1103/PhysRevC.69.055806.

16) Stave, S., Ahmed, M. W., France, R. H., Henshaw, S. S., Müller, B., Perdue, B. A., Prior, R. M., Spraker, M. C. & Weller, H. R. (2011). Understanding the B11(p,α)αα reaction at the 0.675 MeV resonance. Physics Letters, Section B: Nuclear, Elementary Particle and High-Energy Physics, 696(1–2), 26–29. https://doi.org/10.1016/j.physletb.2010.12.015.

17) Tarcan, G., Subaşı, M., Özbir, Y. & Baykal, A. (1998). J-15 Hızlandırıcısının Yeniden Kazanılması. CNAEM Report, TR-335.

18) Wessel, F. J., Binderbauer, M. W., Rostoker, N., Rahman, H. U. & O'Toole, J. (2000). Colliding beam fusion reactor space propulsion system. AIP Conference Proceedings, 504(1), 1425–1430. https://doi.org/10.1063/1.1290961.

19) Whitcher, R. (2014). SaCalc-Ellipsoid.

http://www.oecd.nea.org/tools/abstract/detail/nea-1884.

20) Ziegler, J. F., Ziegler, M. D. & Biersack, J. P. (2010). SRIM - The stopping and range of ions in matter (2010). Nuclear Instruments and Methods in Physics Research, Section B: Beam Interactions with Materials and Atoms, 268(11–12), 1818–1823. https://doi.org/10.1016/j.nimb.2010.02.091.